Impacts of Relaxing Humidity Constraints on Chilled Water Demand in a Commercial Building

Rebecca Grekin [1]*, Jacques de Chalendar [1], Sally Benson[1]

[1]Stanford University, Energy Science and Engineering,
Palo Alto, California, United States
rgrekin@stanford.edu
jdechalendar@stanford.edu
smbenson@stanford.edu

* Corresponding Author

ABSTRACT

In 2018, commercial building space cooling alone consumed 9% of the world's electricity, and the median age of the U.S. commercial building stock was 37 years. Heating, Ventilation, and Air Conditioning (HVAC) systems in older buildings often have limited controls and are expensive to upgrade. Current HVAC operational rules of thumb are outdated and do not prioritize energy efficiency. Here, we explore opportunities to reduce energy consumption in existing commercial buildings by explicitly considering both indoor and outdoor relative humidity (RH) in HVAC operational decision making through real-world experiments.

Air handling unit (AHU) set point temperatures are generally very low (50-55°F/10-12.8°C), to condense excess water from the outside air to maintain indoor RH below 50-60%, well below the maximum RH limits set by ASHRAE Standard 55 for occupant comfort. The air is then often reheated to maintain a comfortable indoor temperature. Relaxing indoor space RH constraints is thus expected to save energy. To quantify these energy savings, experiments were conducted in a commercial building at a corporate campus in Texas (IECC climate zone 2A, Hot Humid). Over the course of three weeks, the AHU Supply Air Temperature (SAT) set point was repeatedly increased from a baseline of 55°F (12.8°C) or 57°F (13.9°C) to 59°F (15°C). There are three main findings from these experiments: indoor RH increased from 55% to 65%, cooling load was reduced by up to 10%, and zone-level temperatures were minimally impacted (+0.45°F/0.25°C). Experimental conditions met ASHRAE Standard 55 comfort levels and maintained no risk of mold growth. We also measured secondary system effects, including the impacts on total air flow and reheat activity. The system was modeled using enthalpy calculations and good agreement was found between measured and calculated chilled water loads. This indicates that a simple model for estimating chilled water load can be created to understand how demand responds to changes in set points if accurate air flow estimates through the system are available. Our results indicate that relaxing RH constraints could significantly reduce cooling loads and provide a lever for demand flexibility, applicable in existing buildings with limited HVAC controls across the U.S.

1. INTRODUCTION

1.1 Demand Flexibility Potential of Commercial Buildings in the U.S.

The potential for increasing energy efficiency and providing demand flexibility of Heating, Ventilation, and Air Conditioning (HVAC) in existing commercial buildings in the United States is large and is important for a number of reasons. Lawrence Berkeley National Lab defines demand flexibility as the capacity of a demand-side load to change their energy consumption patterns on a given timescale (Berkeley Lab Building Technology & Urban Systems Division, 2023). First, commercial building HVAC consumes a large amount of energy. In 2021, 12% of global final energy use was used for heating and cooling commercial buildings (González-Torres et al., 2022), and in 2018 it is estimated that space cooling alone consumed 9% of the world's electricity use (International Energy Agency, 2018). This work focuses on U.S. commercial buildings which include offices, retail sites, supermarkets, schools, laboratories, and data centers, that represented 35% of U.S. electricity sales in 2020 (U.S. Energy Information Administration, 2022a).

The existing commercial building stock in the U.S. and the world is large. In 2018, the median age of the commercial building stock in the U.S. was 37 years, and 21% of buildings were built before 1960 (U.S. Energy Information Administration, 2022b). Experiments in real, as well as in older, buildings are needed because building stock turnover is likely to remain slow, and because there has historically been a discrepancy between real-world measurements and engineering calculations in building modeling (Saad & Eicker, 2023). Although there are often significant energy savings possible from large scale retrofits of older systems, retrofits are expensive. Low-cost alternatives, which leverage as-is HVAC systems are needed because many buildings owners and operators are not willing or able to invest significant upfront capital to reduce operational costs. In addition, incentives are often misaligned when building owners and operators need to pay for expensive retrofits but do not pay the utility bills, and thus do not reap the benefits from upgrading. To achieve a lower carbon future, legacy building stock must reduce energy consumption by, for example, participating in demand response mechanisms. To assess the potential of the existing building stock demand flexibility, demand response, and efficiency improvements, real-world experiments in buildings are needed.

Demand flexibility is an important component of decarbonization because shifting demand allows for the smoothing of the demand curve. By smoothing out this curve, the peaks are decreased, and thus less infrastructure must be built to handle the peak system loads. However, to leverage demand flexibility, it is crucial to know what fraction of a load is flexible. The best way to determine the flexible load in buildings is to conduct experiments and determine what fraction of total load is reduced when demand flexibility tactics are implemented.

This work details experiments which are possible to conduct in older buildings which leverage real-world measurements using existing sensors and control points to find low-cost opportunities for improvements in HVAC energy consumption. This research focuses on finding opportunities "to teach old buildings new tricks." We believe there is an opportunity to find previously overlooked aspects of HVAC systems which represent low hanging opportunities for energy efficiency improvements by carefully considering industry rules of thumb. Most of these rules of thumb were developed in the 1960s and earlier when electricity was relatively inexpensive, and people were not concerned with excess energy consumption. These rules of thumb consider worst-case scenarios and use "set it and forget it" approaches for most of the parameters in the system (Raman et al., 2020). However, worst-case scenarios are not the same everywhere, they are low in frequency, and new perspectives have started to question these industry standards to find low-hanging opportunities for energy reductions.

1.2 Heating Ventilation and Air Conditioning (HVAC) Systems

HVAC systems control both indoor temperature and humidity and a common arrangement for commercial building HVAC systems is illustrated in Figure 1. A commercial site can have electric, steam, or a mix of both types of chillers which produce cold water. The cold water is sent to the buildings where it interacts with air in an air handling unit (AHU). One AHU can service many different thermal zones. Zones are often single rooms, although one room may have several thermal zones depending on design. A mixture of outside air and return air enters the AHU and flows over cooling coils which contain the cold water that is produced by the chillers. If the outside air is very humid, this cooling step in the AHU will condense excess water and constrains indoor air relative humidity.

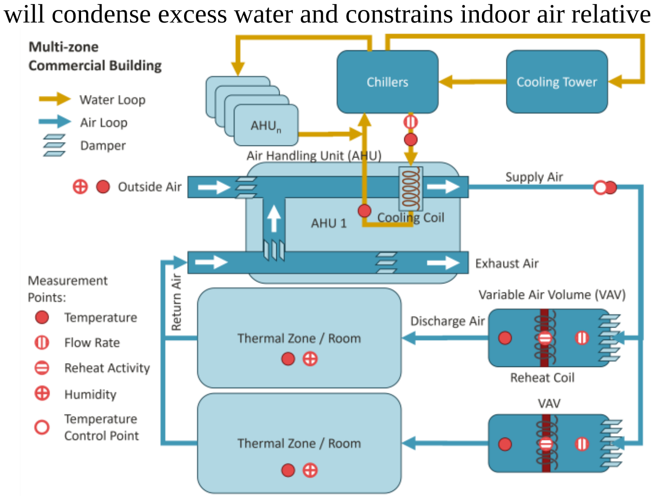

Figure 1. Schematic of a typical HVAC system. Chillers produce cold water which interacts with and cools air in Air Handling Units (AHUs). The cold air then passes through Variable Air Volume (VAV) boxes where the air is often reheated before entering a thermal zone. In this work, the control point is the Supply Air Temperature. Each chiller services multiple AHUs. Humidity measurements were not integrated into the AHU control system and were conducted with a hand-held sensor and building walkthroughs; other sensors were integrated into the system.

The cold air, called supply air, enters a zone through a Variable Air Volume (VAV) or Fan Powered Box (FPB). These units have dampers which control how much of the cold supply air enters a room. VAV boxes also often include a heater which warms the air before it enters the room, if necessary, usually through resistive heating or a hot water or steam coil. Usually, HVAC systems work by cooling down the mixed air in the AHU to between 50°F (10°C) and 55°F (12.8°C) which helps both regulate humidity and temperature (Jerry Williams, 2013). It is often the case that the outside air is cooled down to this low temperature solely for humidity control and for temperature control the air is often reheated in the VAV before entering the room.

The systems discussed in this work are representative of older commercial buildings that do not have modern controls. Modern controls are often required for internet of things (IoT) integration, a common tactic to improve system operations. IoT is defined as "the concept of making devices capable of connecting to the Internet, enabling them to work together to best serve the user" (Zhang et al., 2016). These older buildings without modern controls are that much more difficult to consider in decarbonization and demand reduction plans, but they are still a crucial component of the puzzle. Much research has been dedicated to using top of the line sensors and real time data for building control decision making and these approaches often use IoT techniques. These techniques can be very effective in reducing energy consumption but require expensive retrofits and upgrades to systems which can be difficult to implement in older systems, which are the focus of this work. Oftentimes the types of systems targeted in this work have manual valves that need to be adjusted by hand to change set points which limit the frequency at which set points can be changed and make controls upgrades expensive. Sometimes this is because the system is old enough that the valves are pneumatic, and sometimes the systems are broken such that the digital controls do not work, and manual overrides are necessary. If the system or controls are broken, the manual overrides are cumbersome, but may not cumbersome enough that the building manager has decided to spend the capital to fix the issue when the manual override is sufficient. These are exactly the systems that need significant retrofits and could have a large energy saving potential but have a very low likelihood of retrofits being completed. This work focuses on finding easy, low-cost, actions that can be implemented and still help reduce emissions and energy consumption of these types of systems.

1.3 Humidity Control in HVAC Systems

HVAC systems control both humidity and temperature. The lower the AHU supply air temperature (SAT), the greater the amount of water that is condensed from the air in the AHU. When the dehumidified air is heated back up to room temperature, its relative humidity is much lower than that of the outside air. When the AHU SAT is 50°F (10°C) and 55°F (12.8°C), the relative humidity of that air once warmed to 72°F (22.2°C) would be a maximum of 46.7% and 55.5%, respectively. This range of SAT has been the rule of thumb in HVAC operations because historically the target indoor relative humidity has been 50%. This value has been set as it was historically considered the ideal intersection between occupant comfort, reduced risk of mold growth, and humidity control for electronic equipment.

a.

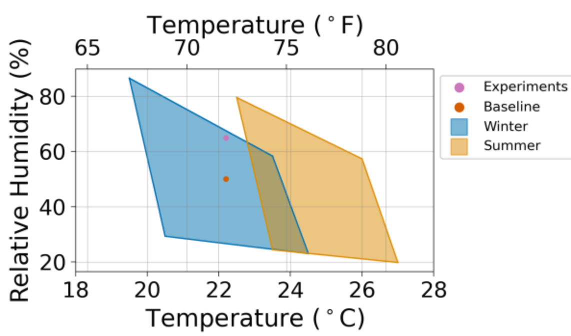

b.

Indoor Conditions at 70°F (21.1°C)

Relative Humidity (%)	Dew Point (°F/°C)	Days to Mold Growth
66	58.0 / 14.4	No Risk
68	59.0 / 15.0	340
70	60.0 / 15.5	163
74	61.0 / 16.1	49
80	63.0 / 17.2	13
85	65.0 / 18.3	6

Figure 2. a. Shaded areas for the ASHRAE Comfort Chart - Standard 55. The red point represents baseline conditions at 72°F (22.2°C) and 50% RH and the pink point represents an elevated humidity of 65% at the same temperature. Adapted from (ANSI/ASHRAE, 2023). **b.** Indoor humidity conditions necessary at 70°F (21.1°C) for there to be significant risk of mold growth. Adapted from (Audits & Consulting, 2015).

Figure 2a. shows the Comfort zone chart developed by the American Society of Heating, Refrigeration, and Air Conditioning Engineers (ASHRAE) for ASHRAE Standard 55 (ANSI/ASHRAE, 2023). The shaded quadrilaterals in Figure 2a. are ASHRAE's definitions for the human comfort range for winter (blue) and summer (orange). The red and pink points in Figure 2a. represents the baseline and experiment conditions of the building studied in this work of 72°F (22.2°C) at 50% relative humidity and 72°F (22.2°C) at 65% relative humidity, respectively. Both conditions are well within the comfort range. Interestingly, the baseline operating conditions of the studied building are outside of the summer range which indicate that there is additional room for energy efficiency improvements in shifting the building baseline operating conditions to better align with the ASHRAE Standard 55 summer comfort conditions.

In terms of mold growth, Figure 2b. illustrates the relative humidity at 70°F (21.1°C) and the number of days at those conditions which are necessary for there to be a risk of mold, mildew, or fungus to grow. For example, if the relative humidity is 68% at 70°F (21.1°C), those conditions would need to remain constant for 340 consecutive days for there to be a risk of mold growth. Thus, there is an opportunity to relax the indoor relative humidity rule of thumb of 50% both on the occupant comfort and the risk of mold growth perspective.

2. RESULTS

Experiments consisted of making chilled water load measurements while alternating the AHU Supply Air Temperature (SAT) between 55°F (12.8°C) or 57°F (13.9°C) and 59°F (15°C). Set points were alternated every 2-3 days as illustrated in Figure 3. AHU 1E, 1W, and 2E had SAT set points of 57°F (13.9°C) and AHU 2W, 3E, and 3W had set points of 55°F (12.8°C). The AHU SAT set point schedule was designed to limit the humidity changes to less than 10% above the baseline value. Two separate zones (East and West) of the building were used in the experiment.

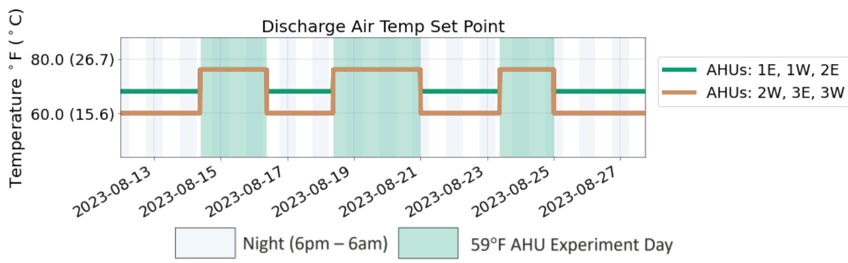

Figure 3. SAT set points for the 6 AHUs in the building. Green sections of the graph represent experiment periods.

2.1 Experimental Results

Increasing the supply air temperature from 55°F (12.8°C) or 57°F (13.9°C) to 59°F (15°C) resulted in increasing the indoor air humidity by approximately 10% as illustrated in Figure 4. The existing HVAC system in the experimental building did not contain integrated humidity sensors, thus building walk-throughs were conducted during experiments to measure the zone-level humidity and temperatures with a handheld sensor. Zone temperatures did not have a large obvious change between experiment (yellow points) and baseline (blue points). The measured relative humidity during experiments remained below 65%, showing that increasing the SAT of the AHUs to 59°F (15°C) successfully increased the RH of the zones by no more than 10% and maintained zone temperatures within normal bounds.

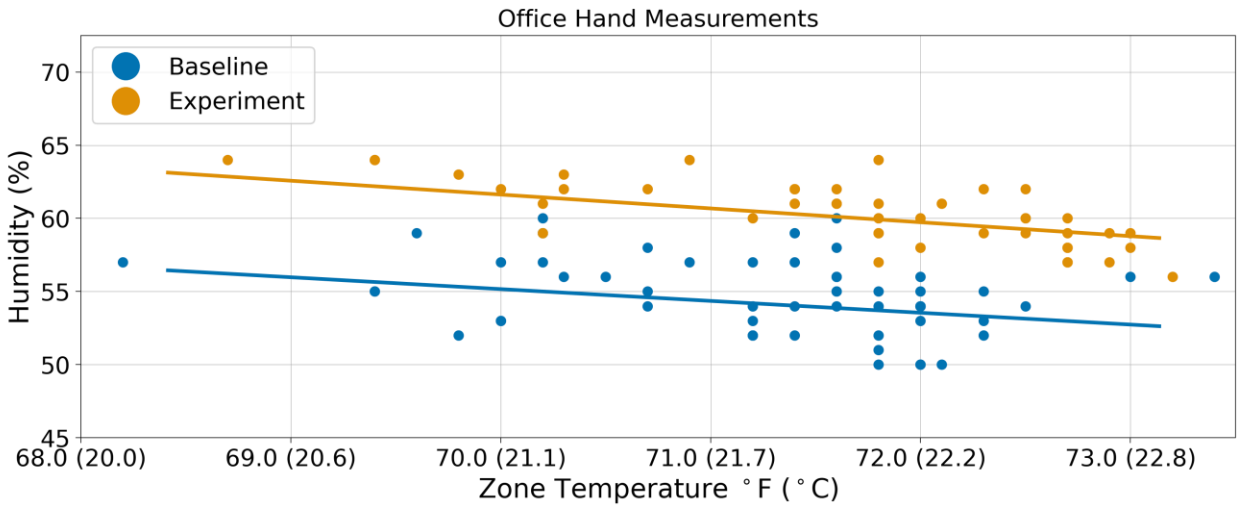

Figure 4. Measured zone temperatures and humidity from building walkthroughs during baseline (55°F/12.8°C or 57°F/13.9°C) and experiments (59°F/15°C).

Figure 5 illustrates the chilled water consumption during the experiment as it relates to outside air enthalpy, which considers both outside air temperature as well as humidity. The best fit line between the experiment and baseline data was found and the overall R^2 value for the data with all 6 AHUs was 0.86 as shown in Figure 5a. The shaded regions represent the 95% confidence interval of the trendlines. Of note, the orange trendlines are below the blue trendlines which indicates that for the same mean daily enthalpy, less chilled water is needed on days with experiments as compared to days without experiments. There is no overlap of the 95% confidence intervals for the experiment and baseline trendlines. There was between 7.5-9% reduction in chilled water demand over the range of observed mean daily enthalpies. An almost 10% reduction in cooling load with a small increase in the air handling unit set point supports the hypothesis that small adjustments to humidity can result in significant energy savings.

Figure 5b. and Figure 5c. show data from the two halves of the building on which experiments were conducted – the East and the West side as illustrated in Figure 9 because cooling demand data was measured for each half separately. Figure 5a. is the sum of Figure 5b. and Figure 5c. and represents the results for the building as a whole. The West side of the building responded more to the experiments with between 8-10% decrease in cooling load as compared to the East side which only saw between 6-7% decrease over the range of observed mean daily enthalpies. The impact displayed on Figure 5 represents the difference in y-intercept between the experiment and baseline regressions.

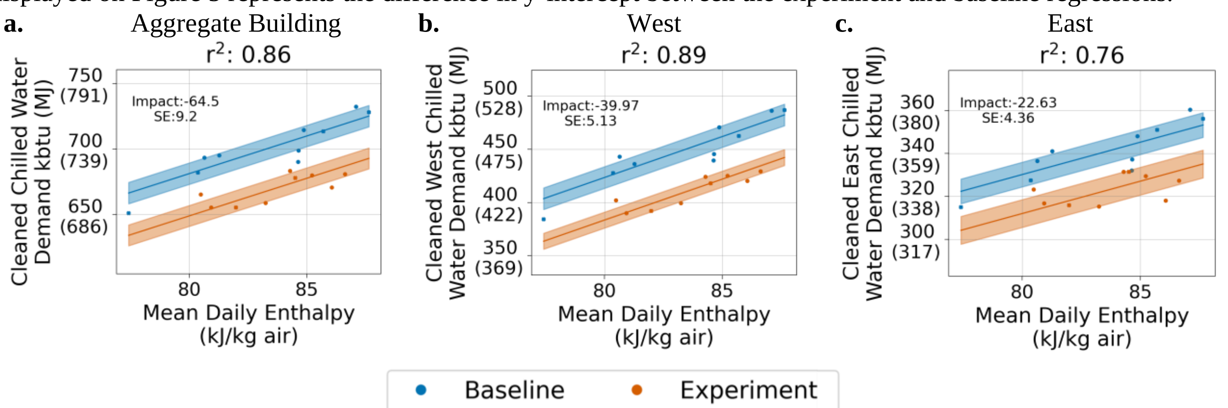

Figure 5. Cooling demand results of three weeks of experiments regressed with mean daily enthalpy. Baseline represents 55°F (12.8°C) or 57°F (12.9°C) SAT depending on the AHU and experiment represents 59°F (15°C) AHU SAT. **a.** represents the aggregate data, and **b.** and **c.** show West and East halves of the building, respectively. Shaded regions represent the 95% confidence interval of the regression trends. The impact represents the change in y-intercept of the trendlines for baseline and experiments and SE is the standard error for the y-intercept impact.

Figure 6 shows the impact of the experiments on other parameters within the system: average zone temperatures, air flow rate, and reheating. During experiments, as illustrated in Figure 6a. zone temperatures were slightly higher than during baseline at about +0.45°F.

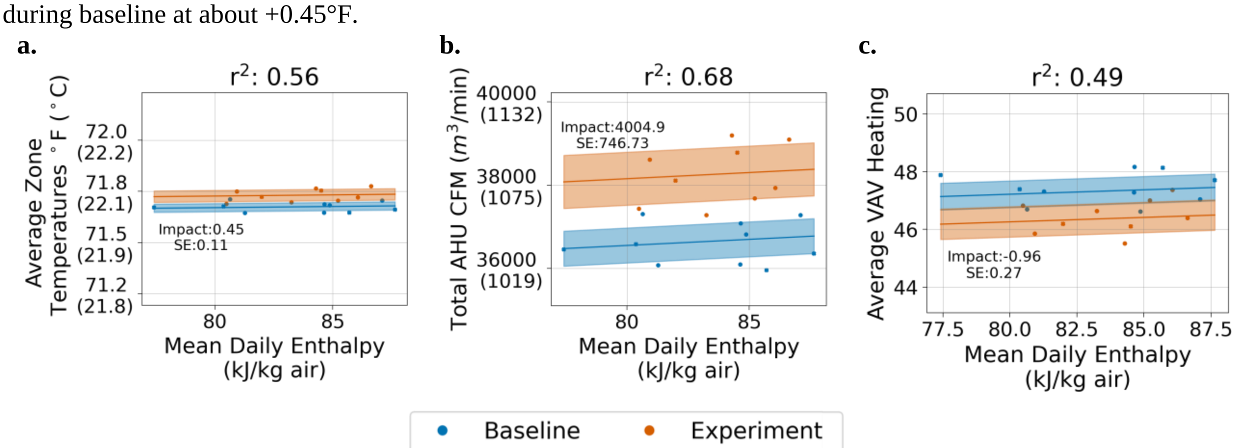

Figure 6. Experiment impacts on other system parameters: **a.** Average Zone Temperatures (°F), **b.** Total Air Flow Rate through AHUs (Cubic feet per minute), and **c.** average VAV reheat activity (%). Shaded regions represent the 95% confidence interval. The impact represents the change in y-intercept of the trendlines for baseline and experiments and SE is the standard error for the y-intercept impact.

Figure 6b. shows the sum of the air flows through all the VAVs. The higher the air flow, the more energy is needed by the fans. There was an increase of approximately 11% in the amount of air flowing through the system during experiments as compared to baseline. Measurements of fan electricity consumption are needed to understand how this increase in fan power affects the overall system electricity consumption. However, the increase in energy needed by the increased air flow is in part counteracted by the decrease in reheat activity illustrated in Figure 6c. The reheat system uses electric resistance heating to reheat the air before it enters a zone if the supply air provided by the AHU is too cold for the zone set point. The reheat in the system is measured at the VAV level in terms of percentage from 0-100%, where 0% means no reheat is being used and 100% means that the heating element is turned on at 100%. Figure 6c shows a simple average of these percentages as a proxy for the reheat activity during experiments and baseline. There was a decrease in reheat which was expected due to the increase in the temperature of the air being provided, but it was relatively small at just a 2% decrease. A decrease in reheat is another potential opportunity to save energy which was illustrated by the results from these experiments.

2.2 Enthalpy Modeling Results

To bridge the gap between engineering calculations and real-world measurements, a simplified model of the HVAC system was developed to estimate the cooling load of the building during the experiment period using enthalpy calculations. Equations (2) through (5) in Section 4. MATERIALS AND METHODS describe the well-defined and understood methods for calculating enthalpy from temperature and humidity values (The Engineering Toolbox. (n.d.). *Moist Air Enthalpy*. https://www.engineeringtoolbox.com/enthalpy-moist-air-d_683.html). Estimating the enthalpies of the outside air, the supply air, and the discharge air, which are highlighted in Figure 7, required humidity values. The system did not have integrated humidity sensors, thus calculated humidity values were necessary.

To estimate the humidities at the AHU SAT and at the zones, it was assumed that the air at the AHU SAT was at 100% relative humidity, and that the amount of water stayed constant once warmed up to the zone temperatures. The outside air humidity was available through a local weather station. The measured zone humidities illustrated in Figure 4 ranged from 50-65% and the estimated zone humidities using the above methods ranged from 50-70%, showing good agreement.

The chilled water demand can be estimated using a simple enthalpy driven model illustrated by Equation (1), where RR is the recycle rate as a fraction, $Flow_{AHU,i}$ is the air flow through the AHU_i in cubic feet per minute, $Flow_{VAV,j}$ is the air flow through the VAV_j in cubic feet per minute, h_{OA} is the enthalpy of the outside air, $h_{AHU\ SAT}$ is the AHU supply air temperature enthalpy, $h_{VAV\ DAT}$ is the VAV discharge air temperature enthalpy, and h_{zone} is the zone enthalpies. All enthalpies are estimated in kJ/kg, and J_i is the number of zones for AHU_i. A total of 6 AHUs and 102 zones are considered in the model.

$$Q_{AHU_i} = \left(\left(h_{OA} - h_{AHU\ SAT,i}\right) * \left((1 - RR) * \left(Flow_{AHU,i}\right)\right) + \sum_{j=0}^{J_i} \left(\left(h_{zone,j} - h_{AHU\ SAT}\right) * \left(RR * Flow_{VAV,j}\right)\right)\right) \quad (1)$$

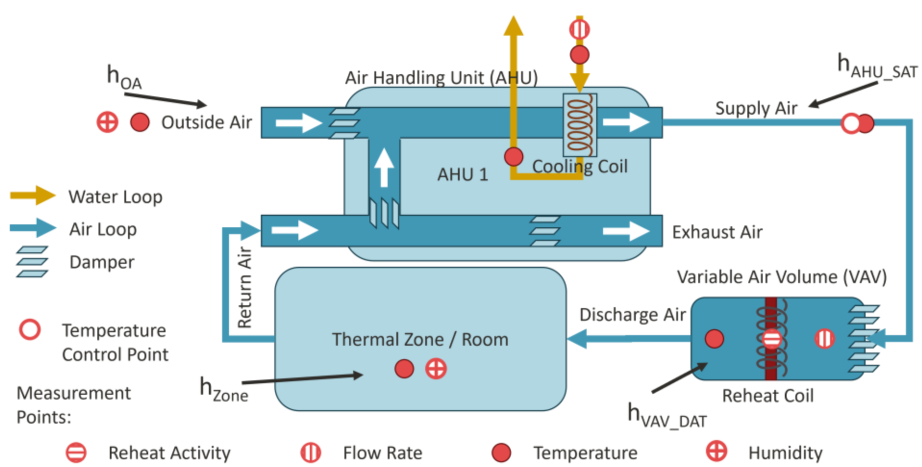

Figure 7. Enthalpy calculations at necessary points in the HVAC System for simplified chilled water demand model.

Figure 8 shows the comparison between the calculated and measured chilled water load during the experiments. Sources of error in the model include the assumption that the amount of water in the air remained constant between the AHU SAT and the zone, errors in total system air flow, and the assumption of no energy losses. It is likely that the amount of water at a thermal zone is higher than that at the outlet of the AHU because of water vapor present in breath when exhaling and other common office occurrences which introduce water into the air, such as boiling water, flushing, and using sinks. In addition, data on temperature and flow through 5 zones was missing due to broken VAV boxes. Thus, the true total air flow through the system is higher than the air flow being used for the estimated chilled water load. In terms of losses, it was assumed that the temperature of the air does not change between the outlet of the thermal zone and the input to the AHU, but it would likely increase at least slightly.

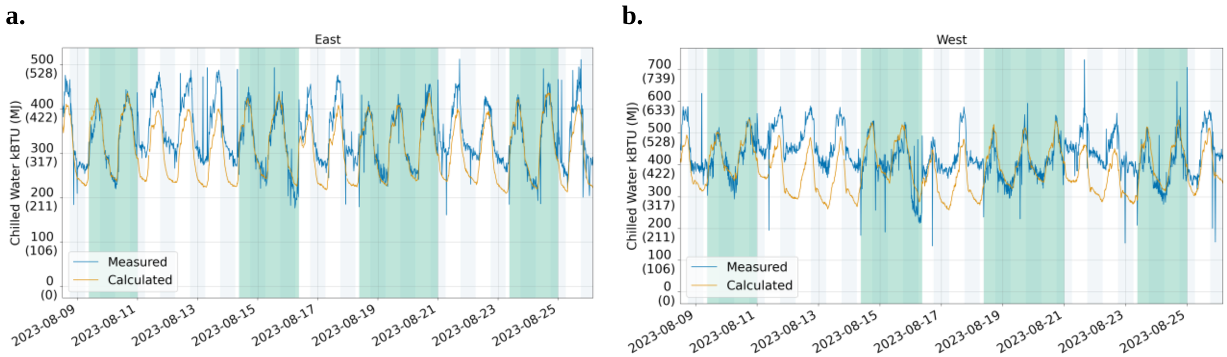

Figure 8. Measured chilled water load from the two buildings sides in blue and calculated chilled water load using methods described above.

The air recycling rate (RR) is also required for Equation (1). Target recycling rates for this building are 90%, however, the best match between the measured and calculated required lower air recycling rates of 70% and 62% for the East and West side of the building, respectively. The East and West side mean absolute errors (MAE) were 11.6% and 15.4%, respectively. However, the error during baseline operations for both the East and West was generally more positive, between 5 and 25%, while the error during experiments was shifted down, between -20 and 10%.

3. DISCUSSION

Up to a 10% decrease in cooling loads was measured during experiments when increasing the AHU supply air temperature to 59°F (15°C) from baseline conditions. This was achieved by allowing an increase in the relative humidity of up to 10%, from the range of 50-56% up to 58 to 65%. This higher humidity range is well within the comfort range for building occupants and sufficiently low to prevent mold growth. Increasing the AHU supply air temperature to 59°F (15°C) from baseline conditions resulted in increasing zone temperatures by only 0.45°F, due to a combination of lowering the amount of reheat and increased fan speeds.

The impact of the experiments on the two halves of the building differed in magnitude, and more experiments are needed to better understand the variables that influence the magnitude of reduction in chilled water load from set point experiments. More analyses are also needed to better understand how the secondary effects (i.e., increased air flow and decreased reheat activity) of the experiments affect overall system energy consumption. For example, if increases in VAV air flow observed during experiments occur in boxes that have reduced reheat activity, the decreased electricity consumption of the reheat coils could negate some, or all, of the increase in electricity consumed by the fans. However, if the increase in air flow is occurring at the VAV boxes where there are also increases in reheat activity, then there is potential for significant increases in electricity due to these two compounding impacts.

It was also found that with accurate measurements of a small number of parameters it is possible to estimate chilled water demand relatively accurately. The required measured parameters are air flow through the VAVs, AHU supply air temperature, zone temperature, outdoor air temperature, and outdoor air humidity, and the required estimated parameters are relative humidity at different points in the system. Much of the literature in HVAC focuses on creating complex physics-based models of buildings and their HVAC systems, which may be impractical for older commercial buildings with limited monitoring data. The results from this work indicate that it may be possible to create relatively simple models for estimating how chilled water demand will respond to changes in controllable operating parameters, such as the temperature set point of the AHU, if accurate estimates of air flow through the different components in the system are available. This simple model can be helpful for evaluating the potential for efficiency improvements and demand response associated with increasing the AHU set point.

The results presented here support the hypothesis that humidity management can be a powerful tool for energy efficiency and demand flexibility, even in older commercial buildings with limited controls. In addition, commercial building HVAC systems can provide a cost-effective demand response mechanism that could significantly reduce strain on and emissions from the grid if understood and leveraged correctly.

The results from these experiments can allow commercial buildings of different vintages to better participate in energy efficiency and demand response initiatives with reduced requirements for capital-intensive upgrades. Standardizing the testing and measurement of commercial building energy performance and demand response in a variety of climates through real world experiments enables more reliable estimates of the energy performance and flexibility of the U.S. commercial building stock.

4. MATERIALS AND METHODS

4.1 Experimental Design

By explicitly considering humidity in the experimental design, these experiments are designed to identify significant opportunities for reduction in chilled water demand by relaxing indoor air humidity constraints. During a three-week period in August, 2023, AHU-level temperature set points were adjusted in 6 AHUs at a corporate campus in Texas (US Climate Zone 2A, Hot Humid) serving approximately 5,850 square meters of floorspace. The building schematic is illustrated in Figure 9. The experiments were run in the East and West sections of the narrow wing which is made up of 3 floors, with the East and West portions being roughly symmetric. The East section has 3 AHUs and 54 zones, and the West section has 3 AHUs and 53 zones. Chilled water measurements including flow rate and temperatures arriving and leaving the sections were available for the East and West portions separately.

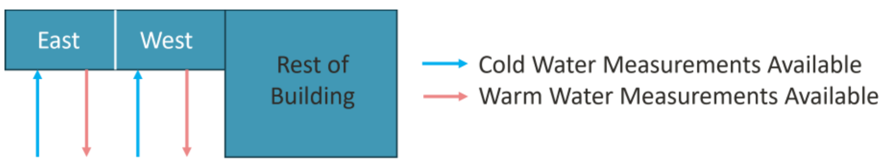

Figure 9. Building schematic. Experiments were conducted in the East and West sections of the narrow wing.

To determine reasonable changes to the system during the experiments, first the baseline conditions of the 6 AHUs in the experimental section of the building were studied. Figure 10 illustrates the baseline Supply Air Temperatures (SATs) of the 6 AHUs in July, the month before experiments were initiated. As shown in Figure 10, AHU 1E and AHU 1W were both unable to maintain their SAT set points before the experimentation period. AHU 1E was fixed and was able to meet its SAT set points during the experimental period. AHU 1W, however, remained broken throughout the experimental period and its AHU SAT often reached temperatures above 65°F (18.3°C). Cases such as this one are typical of the older systems which are targeted by this work; ones in which costly upgrades or retrofits could significantly improve energy consumption, but which the building operators are not willing or able to invest the capital to do so. AHU 1E required a part that was easy to acquire, while AHU 1W required more costly and difficult pieces to attain, and thus was left as-is. It is a goal of this work to show that even in such cases there can still be an opportunity for reductions in energy consumption. Although there is some variance in the SATs of the other 4 AHUs, they were able to maintain their SATs relatively well, as can be seen in Figure 10. The zones serviced by AHU 2E and AHU 2W were unoccupied during the experimental period. Based on these data, it was noted that for the baseline, SAT temperatures were sometimes allowed to climb as high as 63°F (17.2°C), with the temperatures mostly staying below 60°F (15.6°C).

Figure 10. Baseline Supply Air Temperatures (SAT) of the 6 AHUs at the experimental site.

Using the baseline conditions illustrated in Figure 10, the average SAT of each AHU was determined during the observational baseline period. This average SAT was then used to calculate the RH of the zones serviced by these AHUs assuming a zone temperature of 72°F (22.2°C) and that at the AHU SAT conditions the air would be at 100% RH and is illustrated by Figure 11a. It was noted that AHU 1E, while broken, was already reaching an average SAT of 59°F (15°C) and that this would represent an indoor RH of approximately 65%.

The outside air temperature (OAT) and RH at the site were retrieved from a local weather station. The amount of water in the outside air was calculated based on these two parameters using methods described in Section 4.2 and is displayed in Figure 11b. The red line represents the amount of water in air at 100% RH at 55°F (12.8°C), which is the baseline minimum SAT set point of the AHUs. The black line represents the amount of water in air at 100% RH at 59°F (15°C), which is the experiment SAT set point of the AHUs. The 100% RH of the AHU SAT Air assumption mentioned above was made because the amount of water in the outside air illustrated by the blue line in Figure 11b. never crosses the red line, which is the amount of water in air at 59°F (15°C) at 100% RH. With the amount of water illustrated by the red and black lines, when the air is heated to room temperature (~72°F, 22.2°C) it is at approximately 55% RH and 65% RH respectively. This increase represents a 10% increase in RH from AHU 2W, 3E, and 3W baseline shown in Figure 11a of 55% RH. The region shaded in light blue represents all the water that must be condensed when the set point is at 59°F (15°C), and the region shaded in yellow indicates the potential for reduction in condensation possible by increasing the SAT to 59°F (15°C).

The 50-55% RH constraint has been the rule of thumb for HVAC design and operations for decades, but there may be some room for relaxing the constraint for indoor air RH to leverage energy savings from this increase. This relaxation of indoor air RH would allow for less water condensation at the AHU. Although it may seem like a small decrease in the amount of water that needs to be condensed, the phase change from water vapor to condensed liquid water is very energy intense and even this small change in water condensation can translate to large energy savings.

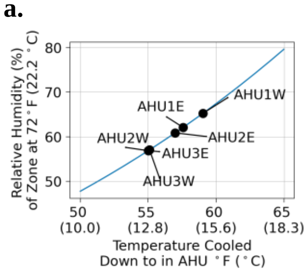

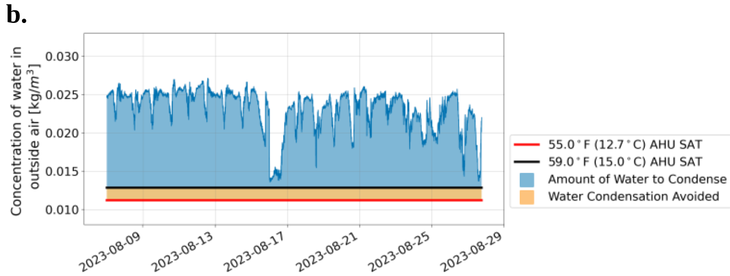

Figure 11. Potential for energy savings. **a.** AHU Average Baseline SATs and the respective zone RHs at those AHU SAT assuming a zone temperature of 72°F (15°C). **b.** Amount of water in outside air, at baseline, and at experiment AHU SATs.

Using back of the envelope calculations considering average AHU air flow rates at the site, it is estimated that more than 16,000 liters per month of water condensation would be avoided by increasing 6 AHU SATs from 55°F (12.8°C) to 59°F (15°C), assuming 20% fresh outside air to the system and an average of 6,750 Cubic Feet per Minute (CFM) of air passing through each AHU. This reduction in condensation is estimated to reduce cooling consumption by 10,125 kWh per month, or a 6.51% reduction in the monthly chilled water demand of the site of 155,495 kWh/month.

Using the data presented in Figure 10 and Figure 11, as well as the previously discussed humidity occupant comfort and mold growth discussion from Figure 2, it was determined that increasing the SAT set point of all AHUs to 59°F (15°C) would be reasonable in terms of maintaining occupant comfort, providing a reasonable possible energy savings, and minimizing mold growth.

Alternating periods of increased SATs and baseline SATs were conducted to increase the chances of similar outside air conditions occurring during experiments and baseline for comparison, and to further reduce the risk of mold growth by alternating between higher humidity periods during experiments and lower humidity periods during baseline. During experiments, the set points were all increased to 59°F (15°C), and during the control periods, the baseline set points for the AHUs were used, either 55°F (12.8°C) or 57°F (13.9°C). In this way, the relative humidity constraints in the zones were relaxed from between 50 and 55% to between 60 and 65%.

4.2 Methods for Calculating Enthalpy and Humidity

The specific enthalpy of moist air, h_{ma}, is described by Equation (2), where h_a is the specific enthalpy of dry air, x is the humidity ratio defined by Equation (3), and h_w is the specific enthalpy of water vapor. The mass of water in the air was determined using steam tables (available through the pyXSteam python library (*PyXSteam · PyPI*, n.d.)), outside air temperature, saturation vapor density, and relative humidity. The other variables in Eq. (3) can in turn be

$$\mathrm{h_{ma}} = \mathrm{h_a} + (\mathrm{x} * \mathrm{h_w}) \tag{2}$$

$$\mathrm{x} = \frac{\text{mass of water vapor}}{\text{mass of dry air}} \tag{3}$$

described by Eq. (4) and (5), where T is the air temperature in °C, $c_{p,v}$ is the specific heat of water vapor at constant pressure defined as 1.86 kJ/kg°C, and h_{we} is the evaporation heat of water at 0°C which is defined as 2,501 kJ/kg. The data for outside air relative humidity and temperature were not available at the building, and thus was retrieved from a local weather station, and introduces a possible source of error.

$$h_a = c_{p,a} * T \tag{4}$$

$$\mathrm{h_w} = \left(\mathrm{c_{p,v}} * \mathrm{T}\right) + \mathrm{h_{we}} \tag{5}$$

REFERENCES

ANSI/ASHRAE. (2023). Standard 55, Thermal environmental conditions for human occupancy. In *American Society of Heating, Refrigerating and Air …*. http://scholar.google.com/scholar?hl=en&btnG=Search&q=intitle:Thermal+Environmental+Conditions+for+Human+Occupancy#0

Audits, N. C. E., & Consulting, B. S. (2015). *Mold Chart for Temperature and Humidity Monitors*.

Berkeley Lab Building Technology & Urban Systems Division. (2023). *Demand Flexibility Service*.

González-Torres, M., Pérez-Lombard, L., Coronel, J. F., Maestre, I. R., & Yan, D. (2022). A review on buildings energy information: Trends, end-uses, fuels and drivers. *Energy Reports*, *8*, 626–637. https://doi.org/10.1016/J.EGYR.2021.11.280

International Energy Agency. (2018). *The Future of Cooling Opportunities for energy-efficient air conditioning Together Secure Sustainable*. www.iea.org/t&c/

Jerry Williams. (2013). *Why is the Supply Air Temperature 55°F?* http://8760engineeringblog.blogspot.com/2013/02/why-is-supply-air-temperature-55f.html

Moist Air - Enthalpy. (n.d.). Retrieved January 8, 2023, from https://www.engineeringtoolbox.com/enthalpy-moist-air-d_683.html

pyXSteam · PyPI. (n.d.). Retrieved January 8, 2023, from https://pypi.org/project/pyXSteam/

Raman, N. S., Devaprasad, K., Chen, B., Ingley, H. A., & Barooah, P. (2020). Model predictive control for energy-efficient HVAC operation with humidity and latent heat considerations. *Applied Energy*, *279*. https://doi.org/10.1016/j.apenergy.2020.115765

Saad, M. M., & Eicker, U. (2023). Investigating the reliability of building energy models: Comparative analysis of the impact of data pipelines and model complexities. *Journal of Building Engineering*, *71*(January). https://doi.org/10.1016/j.jobe.2023.106511

U.S. Energy Information Administration. (2022a). *Electric Power Annual 2020*. www.eia.gov

U.S. Energy Information Administration. (2022b). *2018 Commercial Buildings Energy Consumption Survey Building Characteristics Highlights*. https://www.eia.gov/consumption/commercial/data/2018/pdf/CBECS_2018_Building_Characteristics_Flipbook.pdf

Zhang, X., Adhikari, R., Pipattanasomporn, M., Kuzlu, M., & Bradley, S. R. (2016). Deploying IoT devices to make buildings smart: Performance evaluation and deployment experience. *2016 IEEE 3rd World Forum on Internet of Things, WF-IoT 2016*, 530–535. https://doi.org/10.1109/WF-IoT.2016.7845464

ACKNOWLEDGEMENT

The authors would like to thank the COOLER team, including Maomao Hu, Aqsa Naeem, Ryan Triolo, for their valuable discussions. Funding for this research was provided by ExxonMobil.